ELSEVIER

Chemical Engineering Journal 77 (2000) 43–50

Chemical Engineering Journal

www.elsevier.com/locate/cej

Application of capacitance electrical tomography for on-line and off-line analysis of flow pattern in horizontal pipeline of pneumatic conveyer

K.L. Ostrowski [a,*], S.P. Luke [b], M.A. Bennett [a], R.A. Williams [a]

[a] *Particle and Colloid Engineering Group, School of Process, Environmental and Materials Engineering, University of Leeds, Leeds, Yorkshire LS2 9JT, UK*

[b] *Camborne School of Mines, University of Exeter, Redruth, Cornwall TR15 3SE, UK*

Abstract

Investigation and control of flow phenomena in the pneumatic conveying of solids requires a detailed knowledge on the flow regimes and a number of phase flow properties. Electrical capacitance tomography (ECT) is shown here to be a robust tool for this purpose, particularly when dense phase plug flow is to be monitored. The application of ECT to dense phase powder conveying in an experimental vacuum system is demonstrated and described, including the visualisation of slug size, shape and velocity. Measured gas and solid flow rates were also analysed in an attempt to ultimately provide a basis for comprehensive on-line analysis. A number of statistical estimators were selected and used in data processing, in order to distinguish between particular types of dense flow. The results show the potential for use of the method for the on-line control of dense phase pneumatic conveyors.

Keywords: Tomography; Pneumatic conveyer; Dielectric constant; Control

1. Introduction

Pneumatic conveying offers many advantages over other methods of granular solids transport factors, such as low routine maintenance and manpower costs, dust free transportation and flexible routing. The main disadvantage is the reliance upon empirical procedures for conveyer design, which often result in an unnecessarily high or variable wear rate and power consumption. In addition, product degradation and particle size separation can be major problems [1].

Slug flow regime, when it occurs in the system, has the advantage of a low air requirement and hence energy demand, low pipeline erosion and low product degradation. However, the *control* requirements of such a transportation system are clearly far more acute in respect to the maintenance of flow regime and the prevention of blockage [2].

This contribution presents a continuation of the author's investigations in using electrical capacitance tomography to monitor and control such a system [2–4]. Details on measurement procedure and the method of data processing are given in [5]. Here we present statistical parameters of an enhanced number of measurements. In this analysis, we are limited to perturbations of averaged powder concentration in the pipe cross-section — the normalised dielectric constant $\langle\varepsilon\rangle$.

2. Experimental set-up

The experimental vacuum conveying system is shown in Fig. 1. The system was designed to enable different types of powder flows to be generated in a different but controlled manner. It is a closed loop for solids and an open system for air. In order to facilitate visual observations of the flow regime the horizontal test section (3 m long), was made from transparent pipe (52 mm inner diameter). The rest of the pipeline was made from transparent or opaque PVC, except for two stainless steel bends used to minimise pipe wall attrition. The height difference between the bottom and upper horizontal sections of the standpipe is approximately 2.7 m. Solids sucked from the solid tank were transferred through a standpipe 11 m in length and stored in the vacuum conveyor. Induced air was pushed through a filter and removed by the vacuum pump to atmosphere.

Vacuum is achieved by using a multistage injector driven by air supplied from a compressor. For a compressed air pressure in the pump inlet section equal to approximately 0.5 MPa, the possible maximum vacuum and maximum induced air flow rate were 80 kPa and 0.1 N m^3 s^{-1}, respec-

* Corresponding author. Tel.: +44-013-233-2789; fax: +44-013-233-2781.

E-mail addresses: k.l.ostrowski@leeds.ac.uk (K.L. Ostrowski), sluke@csm.ex.ac.uk (S.P. Luke), r.a.williams@leeds.ac.uk (R.A. Williams).

1385-8947/00/$ – see front matter
PII: S1385-8947(99)00140-0

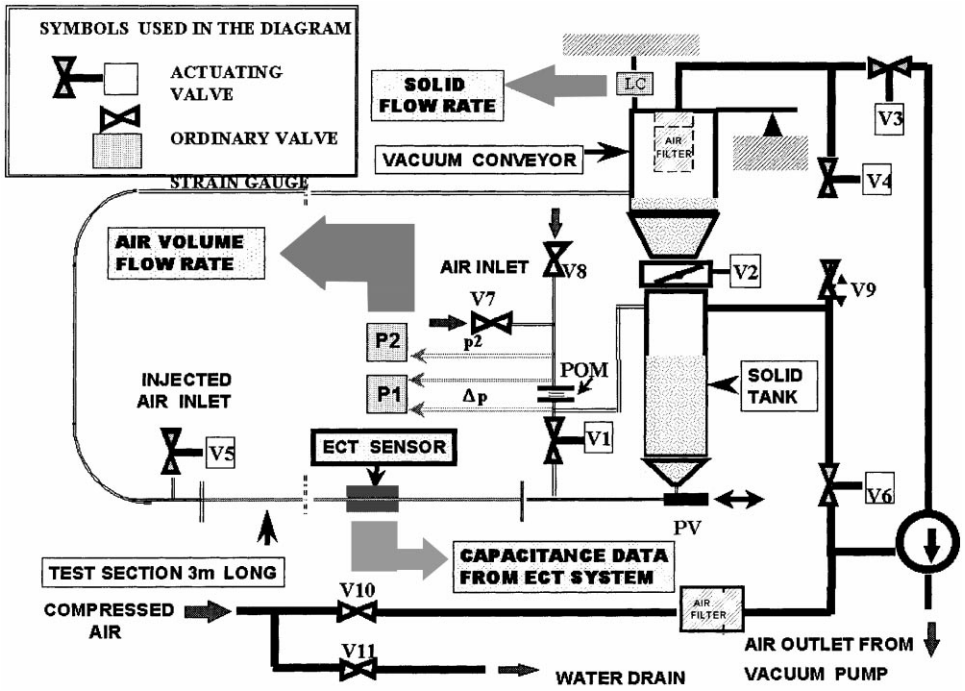

Fig. 1. Experimental set-up.

tively. These parameters were sufficient to generate a wide range of flow patterns, from dense slug flow up to dilute, fast flow (with low solid concentration). The experimental system was operated using eleven valves which controlled the conveying plant and enabled adjustment of the flow parameters which corresponded to particular flow regimes. The valves numbered from V1 to V6 (Fig. 1) were electrically actuated units, and thus, could be operated automatically. The functions of particular valves are listed briefly below, since an understanding of their operation shows how the manipulation of combinations of these valves could be used to produce differing flow regimes.

V1 — main air inlet valve, could be actuated with different frequencies to obtain various slug patterns,

V2 — butterfly valve dividing the vacuum conveyor and the solid tank; when all the solid was transferred through the standpipe, this valve was opened to discharge the vacuum conveyor, otherwise it remained closed during the plant operation,

V3, V4 — auxiliary valves to cut off the system from the vacuum pump and equalising the pressures in the vacuum conveyor and the solid tank,

V5 — injection valve to remove a solid plug from the vertical part of the pipeline (suitable for solids of low fluidity), to feed the system with solids and to generate additional pressure pulses if necessary.

V6, V9 — valves controlling auxiliary bypass which supplied the compressed air directly to the solid tank (suitable for solids of low fluidity),

V7, V8 — ball and needle throating valves which controlled air flow rate,

V10 — compressed air cut-off or throating valve,

V11 — outlet valve to drain water from the compressed air pipeline.

According to the above, the conveying plant flow parameters were adjusted mainly by valves V1, V7, and V8. If necessary, the auxiliary valves V5 and V10 could be used for this purpose (the latter valve to change the vacuum pump characteristics), while valves V2, V3 and V4 controlled the discharging process after solids transfer was completed. Since the conveying plant was designed to examine the flow of different types of powders or plastic pellets, the plug valve (PV — Fig. 1) was mounted at the solids inlet to adjust its cross-section. A detailed description of the system is also given in [5,6].

The material conveyed was nylon plastic pellets having a bulk density of 750 kg m^{-3}, a solid density of 1120 kg m^{-3}, a length of 2–3 mm and an aspect ratio between 1–2. For this medium, the maximum mass transferred during a single run was approximately 25 kg, these being determined by the volume of the solids hopper.

In addition to the data supplied by the electrical capacitance tomography (ECT) system, two other parameters, the gas and the solid flow rates, were measured. Atmospheric air entered the system through valves V7, V8 and then was drawn through an orifice plate flowmeter (OPF). The air stream leaving the orifice plate flowmeter was subsequently split. One stream was directed to the inlet section through valve V1 while the second was supplied to the top of the solid tank and then drawn through the solid packed bed. The ratio of both streams depended on the valve V1 adjustment, on the height of the solid bed in the solid tank and also

on the type of solid. The instantaneous value of total volumetric flow rate was obtained by measurements of pressure drop caused by the OPF restriction and absolute pressure to calculate the fluid density in the orifice plate assembly. These values were provided by two pressure strain gauges P1 and P2 having ranges 2 kPa and 0.1 MPa, respectively. In order to cover as wide as possible range of air flow rates, a set of four orifice plates were fabricated with diameters at the orifice openings equal to 4, 6.2, 7.1 and 12 mm. These corresponded to air flow rates equal to approximately 0.5, 1.2, 2, 5 $N m^3 s^{-1}$ obtained for the maximum pressure drop equal to 2 kPa and the output voltage signal from bridge and amplifier equal to 5 V.

Design of the ECT sensor used for monitoring the flow patterns in the test section was based on the solution of the electrostatic field in the sensing region, described by Ostrowski et al. [7]. Twelve sensing electrodes 100 mm long were supported by two assemblies of guard electrodes. Since the distance required to develop particular perturbations typical for the tested flow regime was a priori unknown, the sensor was movable along the test section, that is, its position versus the inlet section was adjustable.

Images from the ECT systems were reconstructed using a conventional linear back projection, as in the work reported above. These data were used in the statistical and stochastical analysis.

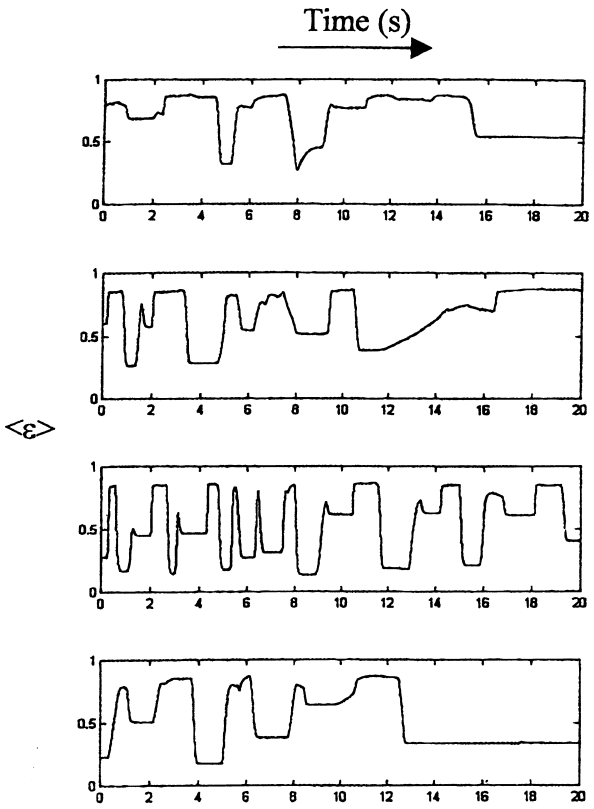

Fig. 2. $\langle\varepsilon\rangle$ (t) signals, from top numbers 1–4. Slow slug flow regime.

3. Results

In the work reported here, reconstructed images can be time-gated to enable quantitative analysis by time-stacking sequential images. The typical information which can be obtained are as follows:

- the average volume occupied by solids
- the height of the solid/gas interface (if present) and then the sequences of images may used to extract [5]:
- slug length and distribution of slug lengths [1]
- slug velocity and velocity distribution[1]
- slug frequency and distribution
- correlation analysis of the above parameters.

As mentioned above in the present analysis we concentrated on the perturbations of the averaged powder concentration in the pipe cross-section, the normalised dielectric constant $\langle\varepsilon\rangle$, obtained as the arithmetic mean value for all pixels (the standard number of them is 814 for ECT system). Such analysis is sufficient to estimate the flow pattern and so provide necessary information for the control procedure.

Within the range of the dense flow regime some sub-regimes may be recognised and defined. Even if air inlet conditions are constant, it is possible to distinguish between *slow* and *fast* (or *dense* and *less dense*) slug flows. The boundary between this two sub-regimes is necessarily artificial. There is however an important point that the fast slug flow has a general tendency to transform into the dilute flow while the slow slug flow demonstrates the trend to block the pipeline.

Additionally, keeping inlet conditions constant and closing and opening periodically another injection valve (in this case Valve 5 in Fig. 1), it is possible to obtained a very regular slug structure – *injected* flow.

Examples of $\langle\varepsilon\rangle$ plotted versus time (in second) for the three slug structures mentioned above are shown in Figs. 2–4. The slow slug regime in Fig. 2 has far longer slugs and a deeper stratified layer (when plugs are not present) than the fast slug flow regime in Fig. 3 where the peaks are sharp and of short duration with a shallow stratified bed For comparison the bottom diagram in Fig. 4 (chiefly demonstrating injected flow) also shows a typical signal for the dilute flow, here the sharp peaks, characteristic of injected plugs in the upper three diagrams, are hardly present, and a certain concentration of powder from the flow can be seen which demonstrates a lower variation than injected flow.

Differences between particular slug patterns are clearly visible. The slow slug flow is more regular than the fast slug flow (generally, the fast slug flow represents the more *disordered* structure compared with the slow slug flow). The two top diagrams in Fig. 4 shows the tendency for blockage to occur typical for this structure. It is also characteristic that the bottom level of solid for all presented signals is not constant but rather a random variable.

[1] In combination with additional data, for example, video images.

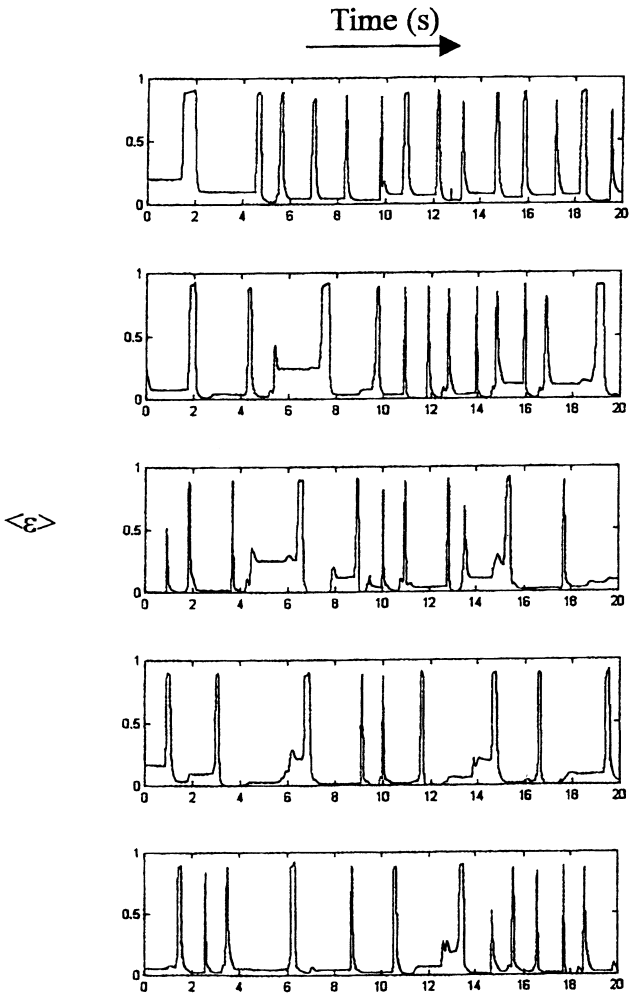

Fig. 3. $\langle\varepsilon\rangle$ (t) signals, from top numbers 6–10. Fast slug flow regime.

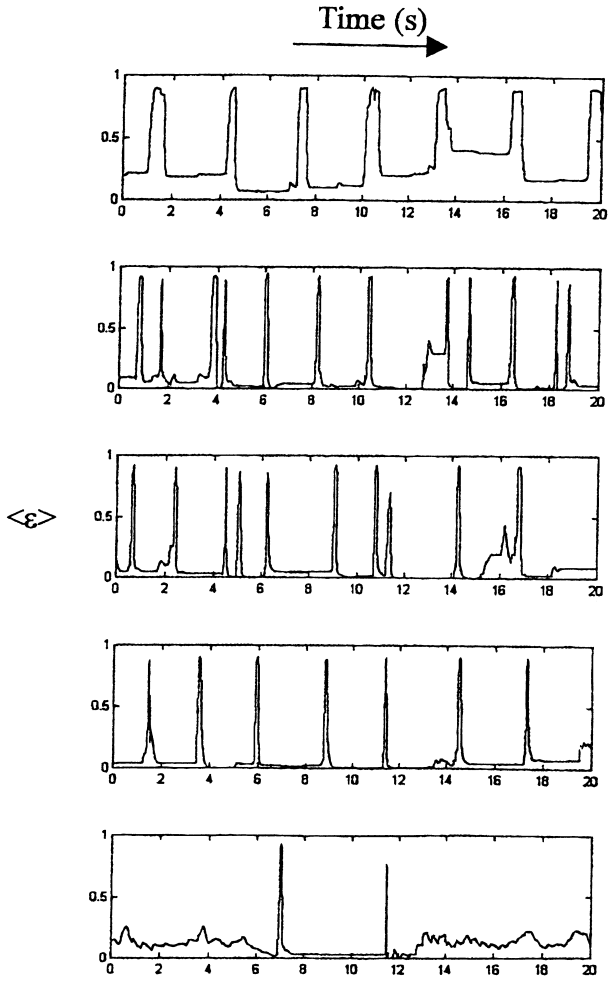

Fig. 4. $\langle\varepsilon\rangle$ (t) signals, from top numbers 11–15. Injected regime and dilute flow (bottom).

Table 1 presents a set of basic statistical parameters for each signal. A summary of flow conditions for the fast and slow slug flows is given in Table 2. The flow parameters (i.e. air and solid flow rates and their superficial velocities) shown in Table 2 do not provide clear information to distinguish particular slug patterns, and so are rather useless for control of the system. Such information, however, is provided by the statistical parameters, namely, the normalised mean dielectric constant, its standard deviation and mean. The standard deviation of the signal yields clear differentiation between any slug flow and dilute flow (or blockage). Median calculation is a prompt tool to differentiate between slow and fast slug flow patterns. Thus the on-line control procedure can be based on these two estimators only.

If off-line analysis is possible, it is reasonable to complete a more comprehensive estimation including autocorrelations, power spectra and histograms of the signals. Examples of these are shown in Figs. 5 and 6.

Fig. 5a–f shows examples of autocorrelation functions (top) and power spectra (bottom) calculated for all types

Table 1
Flow regimes corresponding with the signals $\langle\varepsilon\rangle$ (t) shown in figures and the basic statistical parameters of these signals

No.	Flow regime	Mean value of $\langle\varepsilon\rangle$	Median of $\langle\varepsilon\rangle$	St. dev. of $\langle\varepsilon\rangle$
1	Slow slug	0.70	0.77	0.16
2	Slow slug	0.66	0.72	0.20
3	Slow slug	0.53	0.59	0.25
4	Slow slug	0.51	0.38	0.22
5	Slow slug	0.51	0.44	0.24
6	Fast slug	0.17	0.08	0.24
7	Fast slug	0.16	0.08	0.23
8	Fast slug	0.13	0.04	0.21
9	Fast slug	0.12	0.04	0.21
10	Fast slug	0.10	0.04	0.19
11	Injected	0.30	0.20	0.26
12	Injected	0.11	0.04	0.21
13	Injected	0.10	0.04	0.19
14	Injected	0.08	0.04	0.16
15	Dilute	0.11	0.11	0.09

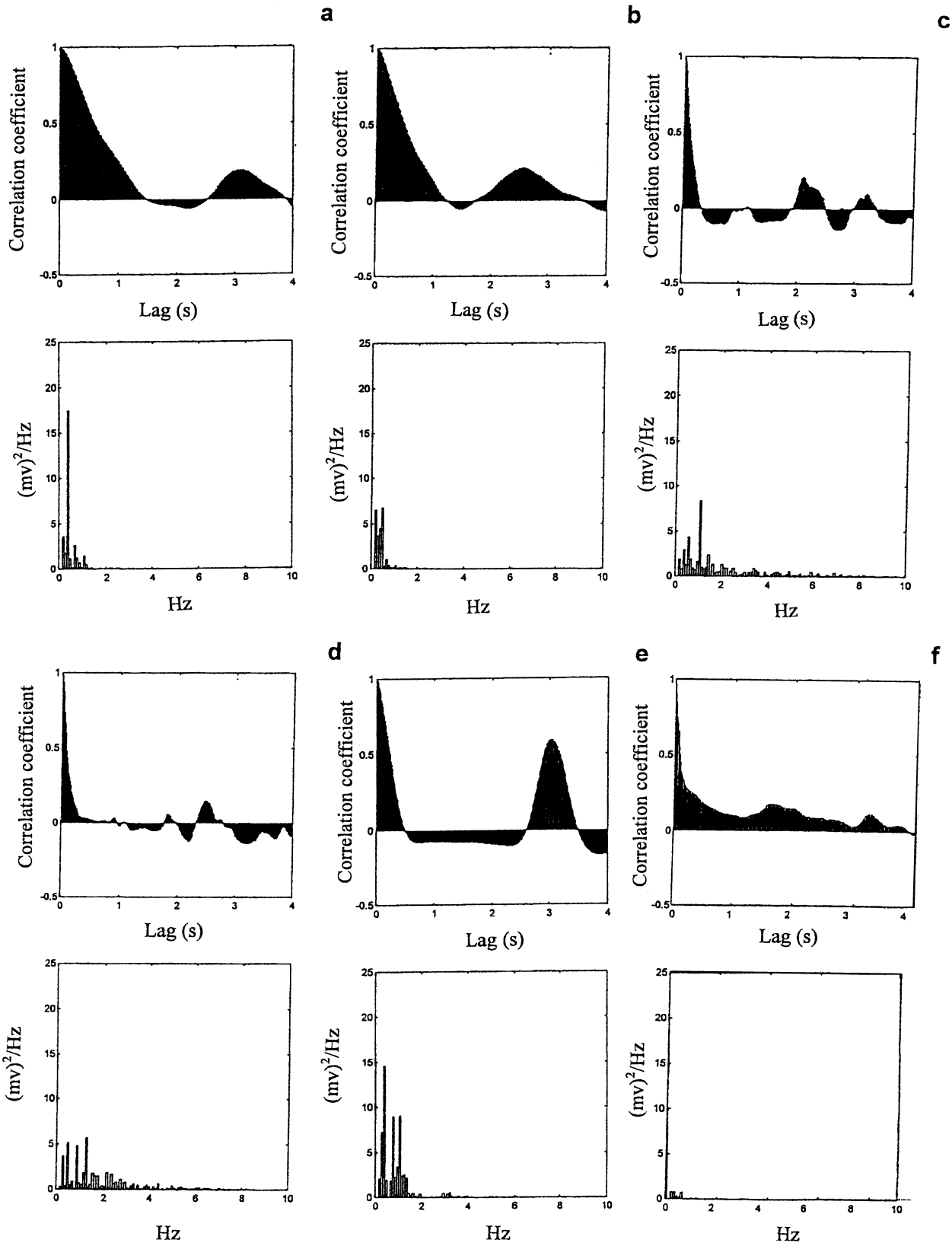

Fig. 5. Autocorrelations (top-lag in seconds) and power spectra (bottom-frequency in 1/s) of some signals listed in Table 1: (a,b) slow slug flow (numbers 1 and 2, respectively); (c,d) fast slug flow (numbers 7 and 8, respectively); (e) injected flow (number 11); (f) dilute flow (number 15) in the power spectrum diagram scale of abscissa is the same as for other pattern to point out the small value of the amplitude for this structure.

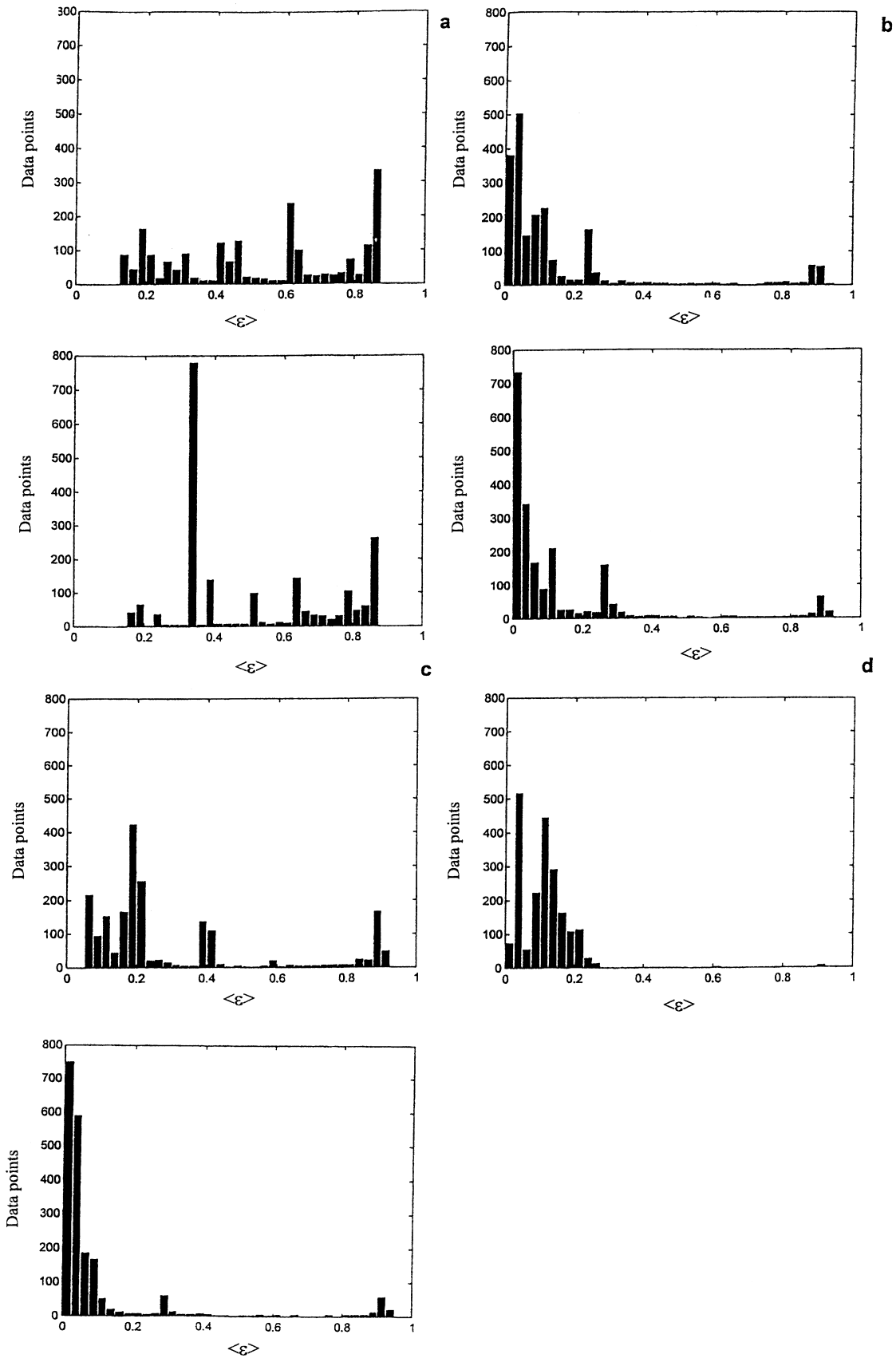

Fig. 6. Examples of histograms for particular structures: (a) slow slug flow, number 1 (top) and 3 (bottom); (b) fast slug flow, number 7 (top) and 8 (bottom); (c) injected flow, number 11 (top) and 12 (bottom); (d) dilute flow, number 15.

Table 2
Air and solid flow rates and the superficial velocities for selected number of the fast and slow slug flows listed in Table 1

No.	Air flow rate ($m^3\,s^{-1}$) $\times 10^3$	Air superficial velocity ($m\,s^{-1}$)	Solid flow rate ($kg\,h^{-1}$)	Solid superficial velocity ($m\,s^{-1}$)
1	0.89	0.42	1370	0.16
2	0.48	0.23	1210	0.14
3	0.70	0.33	1320	0.15
4	0.79	0.37	1370	0.16
6	0.87	0.41	1410	0.16
7	0.89	0.42	1440	0.17
8	0.93	0.44	1480	0.17

of flow. It is clear that the *macroscales* as well as the *microscales* are larger for slow slug flow by about one order of magnitude when compared to the others, indicative of the slower nature of the flow. The injected flow is characterised by relatively high repeatability of the signal (Fig. 5e) resulting from the repeatable nature of the injections. Thus, calculation of autocorrelation is a simple, effective and robust tool to distinguish between particular dense flow patterns. If the slug's frequencies are to be considered, it is more suitable to calculate power spectral density of the signal. Since the spectral *leakage* is generally present, it is therefore common practice to *taper* the original signal $\langle\varepsilon\rangle$ before transformation, reducing any discontinuities at its edges, as discussed elsewhere [5]. The power spectra presented were calculated using data tapering and then the Fast Fourier Transform. The slow slug flow is characterised by a small power spread with a distinctive strong peak at about 0.3 Hz, which would be expected due to its low frequency. Frequency components above 1 Hz may be neglected. The fast slug flow, with its generally high frequency of slugs produces a wider spread, up to 3 Hz, with a few maxims. Injected flow is of a similar frequency to fast slug flow, and so, its power spectra is generally closer to that obtained for the slow slug flow. All power spectral densities calculated for this flow regime (not shown here) are similar to each other and there is no clear dependence of their shape on the phase's flow rates within the ranges tested in present experiment.

Examples of the histograms for flow regimes being tested are shown in Fig. 6. The range of $\langle\varepsilon\rangle$ equal to $\langle 1, 0\rangle$ was subdivided into 100 quantisation levels. These estimators are also different. For the slow slug flow as plotted in histogram form in Fig. 6a the distribution of probability is more symmetrical showing the range of powder concentrations being both high and low, however, the random character of the solid levels is clearly visible. Also, the $\langle\varepsilon\rangle$ distributions are close to *bimodal* (i.e. representing the minimum and maximum solid levels). It is seen that the slow flow represents a more symmetrical distribution than the fast flow. For the former, the maximum probability occurs from relatively high values of $\langle\varepsilon\rangle$, due to the slow passing of dense slugs and a high stratified bed, while for the latter, low solid levels are more probable due to the short duration of slugs in the sensing region compared to a low stratified bed.

The injected flow represent a mixed structure for which both distributions are possible, dependent on the mode of valve operation. Histograms for the dilute flow shows significant nonuniformity resulting from the gravity force and chiefly a high probability of low values due to the low solids concentration in the pipe for the majority of the measurement.

It would of course be possible to extend the number of estimators and include, for example, higher order moments: *skewness* and *kurtosis* as the additional tests. However, we found that none of these provide a clearer method of flow pattern recognition.

The work and principles that have been described, are now extended for on-line control of conveyors with special regards to the prompt identification of flow regime and the quantitative estimation of statistical parameters.

4. Conclusions

The work described here demonstrates the preliminary application of *ECT* to some industrial scale problems. The use of *ECT* for modelling of complex powder flow in dense phase powder flow is potentially a fruitful area. The use of the methodology for on-line control is also promising and industrial examples seem likely to emerge in near future. This will require further and integrated development of the sensor systems and process control systems using model-based reconstruction algorithms where possible and fusion of tomographic data with other conventional multi-sensor data.

Acknowledgements

The author acknowledge the financial support of EPSRC and Camborne School of Mines Trust in different aspects of the work reported here.

References

[1] G.E. Klinzing, R.D. Marcus, F. Rizk, L.S. Leung, Pneumatic Conveying of Solids, 2nd Edition, Chapman and Hall, London, 1997.

[2] S.L. McKee, R.A. Williams, T. Dyakowski, T. Bell, T. Allen, Solid flow imaging and attrition studies in a pneumatic conveyor, Powder Technol. 82 (1995) 105–113.
[3] T. Dyakowski, R.B. Edwards, C.G. Xie, R.A. Williams, Application of capacitance tomography to gas–solid flows, Chem. Eng. Sci. 52 (1997) 2099–2110.
[4] S.J. Wang, T. Dyakowski, C.G. Xie, R.A. Williams, M.S. Beck, Real time capacitance imaging of bubble formation at the distributor of a fluidised bed, Chem. Eng. J. 56 (1995) 95–100.
[5] K.L. Ostrowski, S.P. Luke, M.A. Bennett, R.A. Williams, Real time visualisation and analysis of dense phase powder conveying, Powder Technol. 102 (1999) 1–13.
[6] M.A. Bennett, Ph. D. Thesis, University of Exeter.
[7] K.L. Ostrowski, S.P. Luke, R.A. Williams, Application of conjugate harmonics to electrical process tomography, Meas. Sci. Technol. 7 (1996) 316–324.